Engineering Chemistry
ISSN: 2813-6535, Vol. 7, pp 79-88
doi:10.4028/p-tHtN4C
© 2024 The Author(s). Published by Trans Tech Publications Ltd, Switzerland.
Submitted: 2023-12-02
Revised: 2023-12-29
Accepted: 2023-12-29
Online: 2024-06-26

Effect of Doping ZnO on Activated Carbon Prepared from Waste Paper for Photocatalytic Applications

Jauharatul Wardah[a], Sugeng Winardi[b], Suci Madhania[c], M. Irwan Fatkhur Rozi[d], and K. Kusdianto[e*]

Department of Chemical Engineering, Institut Teknologi Sepuluh Nopember, Kampus ITS Sukolilo, Surabaya 60111, Indonesia.

[a]jauharatul21wardah@gmail.com, [b]swinardi@chem-eng.its.ac.id, [c]wigaviola@chem-eng.its.ac.id, [d]irwan@its.ac.id, [e*]kusdianto@chem-eng.its.ac.id.

Keywords: Activated Carbon, AC/ZnO, Methylene Blue, Photocatalyst, Waste Paper

Abstract. Accumulation of untreated and unrecycled paper has a negative impact on the environment. Like liquid waste handling, paper waste handling is also still being developed. It is known that activated carbon (AC) is one of the promising adsorbents that can be used to solve the environmental issue. Activated carbon can be made from organic waste, such as waste paper. The objective of this study is to investigate the operation condition of the pyrolysis process to obtain the activated carbon. The furnace temperature was set at 400◦C for 1 hour under N_2 stream with a flow rate of 0.5 L/min. To provide a synergistic effect in the adsorption process, ZnO was derived from $ZnCl_2$ as a chemical activator for making active carbon. While $Zn(CH_3COO)_2.2H_2O$ with different concentrations of 0.01, 0.05, and 0.1 M was grown into the pores of activated carbon. The photocatalytic activity of AC/ZnO was identified in the degradation process of methylene blue as a model of organic pollutants. X-ray diffraction (XRD), scanning electron microscope (SEM), and fourier transform infrared (FTIR) were used to characterize the product. The morphology of ZnO was observed in the form of a flower-like and occupying the surface of activated carbon. The photocatalytic activity showed that the methylene blue was completely degraded.

Introduction

Numerous scholars continue to be interested in environmental issues since they appear to have no end in sight. The link between garbage produced by cities and companies and environmental issues is not new [1]. Waste discharged into public rivers frequently has been found to contain various metals, colors, and even harmful microorganisms [2]. In addition to the persistent challenges of liquid waste management, the annual accumulation of millions of tons of untreated and unrecovered paper and its byproducts has emerged as a significant and pressing concern [3]. The majority of waste paper originates from wood or cotton pulp, primarily composed of cellulose fibers (constituting 90-99%), which are rich in carbon, possess a distinctive pore structure, and feature functional groups such as carboxylic and hydroxyl groups [4]. Addressing the mitigation of pollutants carried by effluents requires effective adsorbents like zeolites, activated carbon, activated alumina, silica gel, among others [5]. Activated carbon is particularly favored due to its commendable performance. Furthermore, given the abundant availability of waste paper, which inherently contains carbon-rich components, the synthesis of activated carbon from waste paper presents an appealing option, characterized by high efficiency and effectiveness [6].

The synthesis of activated carbon with high specifications, good structure and pore size is generally done through carbonization and activation processes [7]. Carbonization is part of the pyrolysis process, which involves the thermochemical decomposition of organic materials under controlled conditions, typically in a low-oxygen or oxygen-free environment [8]. During this process, organic matter found in the biomass substrate begins to break down, commencing at temperatures around 350-550 °C and extending up to 700-800 °C [8]. Pyrolysis has the capacity to transform lignocellulosic biomass, encompassing cellulose, hemicellulose, and lignin components, into a spectrum of solid, liquid, and gaseous products. The main products from pyrolysis are non-

This article is an open access article under the terms and conditions of the Creative Commons Attribution (CC BY) license
(https://creativecommons.org/licenses/by/4.0)

condensable gas (e.g., CO, H_2, and CO_2), light hydrocarbons (e.g., CH_4, C_2H_4), condensable gas (tar), solid residue (char), and mineral ash [9].

In the carbonization process, activated carbon is generated through activation, which can be achieved by either chemical or physical means. Physical activation entails the use of activation gases like steam, CO_2, or specific compounds. However, this method, despite being environmentally cleaner, is associated with prolonged activation times, lower production yields, and higher costs [10]. Conversely, chemical activation is typically favored due to its simpler process and more effective activation outcomes [9].

Aluminum chloride ($AlCl_3$), potassium hydroxide (KOH), sodium hydroxide (NaOH), phosphoric acid (H_3PO_4), and other activating agents are commonly employed in activated carbon production due to their benefits, such as low heating temperatures, short processing times, high carbon yields, precise pore control, and increased surface areas [11]. The most popular activating agent among them for the production of activated carbon is the alkali ZnCl2. When it comes to raw materials, ZnCl2 is a more effective dehydrating agent than carbonized materials, which have lost water and volatiles during the carbonization process. [12].

The efficiency of activated carbon in eliminating contaminants from contaminated water has been recognized [13], but the absorption ability of activated carbon under UV light has not been widely studied. Velo-Gala et al. (2013) when exposed to UV light, activated carbon exhibits photoactive and semiconductor properties [14]. On the other hand, Cruz et al, (2017) mentioned that producing composite materials with combined or synergistic features like high surface area, mechanical strength, thermostability and insolubility, antibacterial capacity, and photocatalytic properties will be possible by growing semiconductors onto activated carbon [2].

The semiconductor that is often trusted to be used in various applications including water treatment is ZnO nanoparticles with the advantages of low price, wide band gap of 3.37 EV, high stability, environmentally friendly, and reusable [5]. However, due to the size and weak compatibility of ZnO causing aggregation and one of its lack is the low charge separation efficiency [15]. Many studies have described strategies to lower the rate of electron recombination in ZnO in order to boost its photocatalytic activity recently [16]. It has been claimed that the element C found in activated carbon lowers the band gap energy of semiconductors with large band gaps. ZnO will produce intermediate energy levels in its band gap when C is added, which will lower the material's absorption energy [17]. Thus, incorporating C on ZnO has the dual application of lowering the electron-hole recombination rate and restricting the band gap energy, which in turn causes ZnO's photo-response to shift from the UV to the visible area [18].

Materials and Procedure

Material and Experimental Set Up

In pretreatment for activated carbon synthesis, ≥85% purity of ethanol as waste paper cleaner. The precursor solutions used were zinc chloride ($ZnCl_2$) (E. Merc, D-7646 Darmstadt FR Germany), zinc acetate dihydrate ($Zn(CH_3COO)_2.2H_2O$) (E. Merck, D-5970 Darmstadt, FR Germany) and the substance determined as the pollutant was methylene blue (MB) ($C_{16}H_{18}ClN_3S$).

For the synthesis of activated carbon, chemical activation was taken as a single process where carbonization and activation were carried out at the same time. Waste paper that has been pre-treated using ethanol and water is impregnated using $ZnCl_2$ as a chemical activator at a ratio of 1:1 (wt%) and dehydrated in an oven at 130 ◦C for 5 hours. The pyrolysis process starts by placing the material in a pyrolysis reactor (ceramic boat) which will be inserted into a tubular furnace as a place to burn at 400 ◦C for 1 hour under an N_2 gas flow rate of 0.5 L/min. The use of N_2 is necessary to maintain an inert atmosphere during pyrolysis and help equalize the formation of activated carbon pores. The activated carbon that has been produced is washed using 0.1 M HCl and water until the pH is neutral, then drying for 24 hours at 80 °C in an oven. In this study, the yield of activated carbon derived from waste paper was 80%.

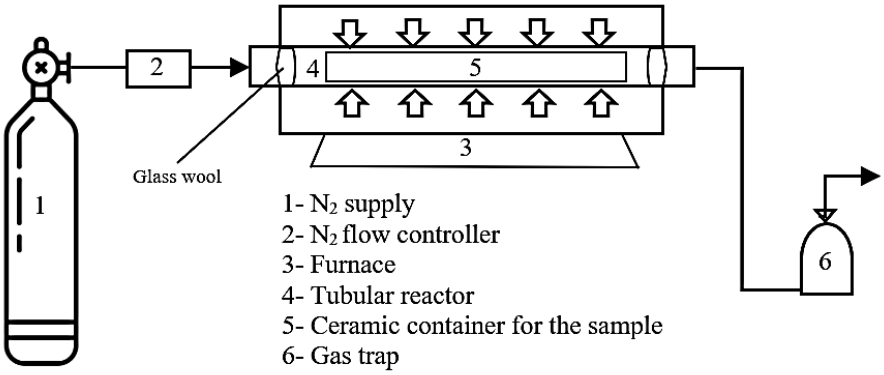

Fig. 1. Schematic representation of the synthesis of activated carbon using furnace pyrolysis method

ZnO NPs were prepared from zinc acetate ($Zn(CH_3COO)_2.2H_2O$) in 100 ml proportions of 0.01; 0.05; and 0.1 M, respectively. The solvent used to dilute the zinc acetate solid was distilled water while the solution chosen to adjust the pH to 8-9 was sodium hydroxide (NaOH) 0.5 M. 5 grams of activated carbon were added to the solution and thoroughly mixed. The mixture was then homogenized for 2 hours while being vigorously stirred, and it was dried for eighteen hours at 80°C.

Methylene Blue Degradation Experiments

The photocatalytic analysis was conducted under one predetermined condition, i.e. enclosed room and without light and only given ultraviolet (UV) light being used as an irradiation source. The UV lamp used was EVACO with specifications of 220V; 50Hz; T8 10W; 365 nm with a maximum intensity of 1190 lux. Before the photocatalytic treatment started, stirring was carried out at 250 rpm for 30 minutes to achieve adsorption-desorption equilibrium conditions. The conquest time of photocatalyst to methylene blue solution lasted at 15-75 minutes with constant stirring. A centrifuge (One Med 0805-I) at 2000r/min for 3 min was used to separate the supernatant from the solid at each analysis interval (15 min). The absorbance was measured using a UV-Vis spectrophotometer at 665 nm [19] for methylene blue. Degradation methylen blue was estimated based on Eq. (1).

$$\text{MB degradation efficiency (MDE)} = \frac{C_0 - C_t}{C_0} x100\% \quad (1)$$

where C_0 and C_t correspond to the initial concentration of MB and following radiation at a specific time (t), respectively. The dye concentration (mg/L) is represented by x in the MB standard linear regression eq. (2), and the absorbance is represented by y.

$$y = mx + c \quad (2)$$

Material Characterization Methods

Utilizing a scanning electron microscope (SEM) (FlexSEM1000, Hitachi High Technologies, Tokyo, Japan), the microstructure of activated carbon derived from waste paper was examined. Using energy dispersive spectroscopy (EDS)-equipped scanning electron microscopy, the composition of various elements on the surface of the AC/ZnO adsorbent was determined. The Philip XPERT MPD, manufactured by Philips and located in Almelo, The Netherlands, uses X-ray diffraction to obtain information about the crystalline structure of the sample. Using the Scherrer equation on Eq. (3), the X-ray line broadening method was used to calculate the material's crystal size (D).

$$D = \frac{k\,\tau}{\beta\, cos\theta} \quad (3)$$

Where k is the Scherrer constant which has the number 0.94, τ is the X-Ray wavelength which has a value of 1.54178 A, β is full width half maximum (FWHM) which is the maximum width of the peak at the total height of the peak and is the angle bragg.

Thermo Scientic Nicolet IS10 Fourier-transform infrared spectroscopy was utilized to identify the functional groups in waste paper-based activated carbon. Tests using infrared spectroscopy were conducted between 500 and 4000 cm^{-1}.

Results and Discussion

Activated Carbon (AC) and AC/ZnO Characterization

Fig. 1 represent a micrograph of the activated carbon made from waste paper, demonstrating the high porosity of the material. The use of $ZnCl_2$ is responsible for the high abundance of pores that are produced [3]. It is believed that $ZnCl_2$ catalyzes the aromatization and rearrangement reactions that result in the formation of carbon and significant amounts of H_2O and H_2. $H[ZnCl_2(OH)]$, which is created when H_2O and $ZnCl_2$ react, further encourages the synthesis of carbon, H_2O, and CO_2. A large number of pores form on the carbon as a result of the material being cracked by $ZnCl_2$ at 400◦C and the release of small molecular gases like CO_2 and H_2O [11].

ZnO is produced during the pyrolysis process by the chemical activator $ZnCl_2$ [2]. It was discovered that the resultant ZnO resembled flowers. The zinc chloride solvent was found to be the chemical activator for this flower-like shape, and zinc acetate dissolved in distilled water was found to be the precursor of ZnO nanoparticles in the amounts of 0.01, 0.05, and 0.1 M [20].

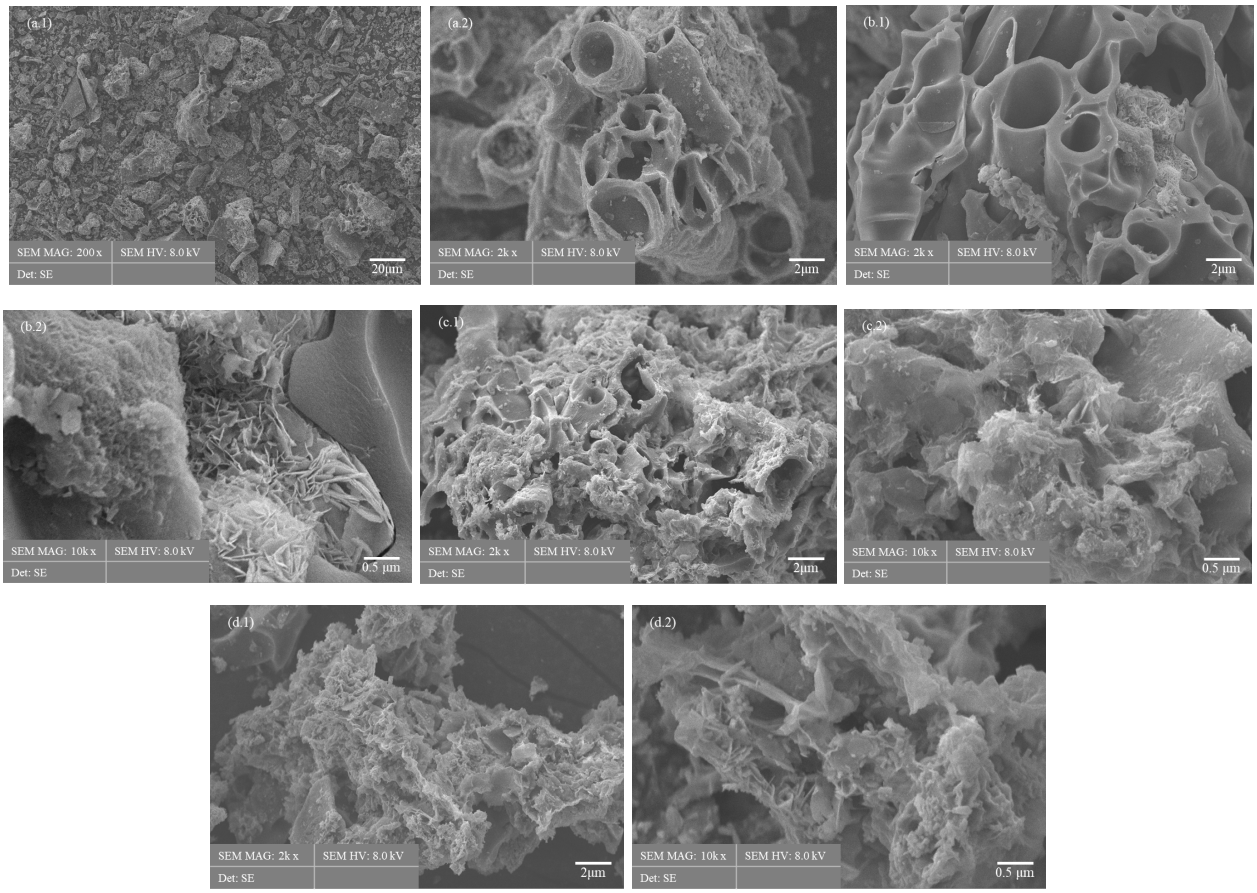

Fig. 2. SEM of activated carbon and doping ZnO (a.1, a.2) activated carbon (b.1, b2) AC/ZnO 0.01 M (c.1, c.2) AC/ZnO 0.05 M (d.1, d.2) AC/ZnO 0.1 M

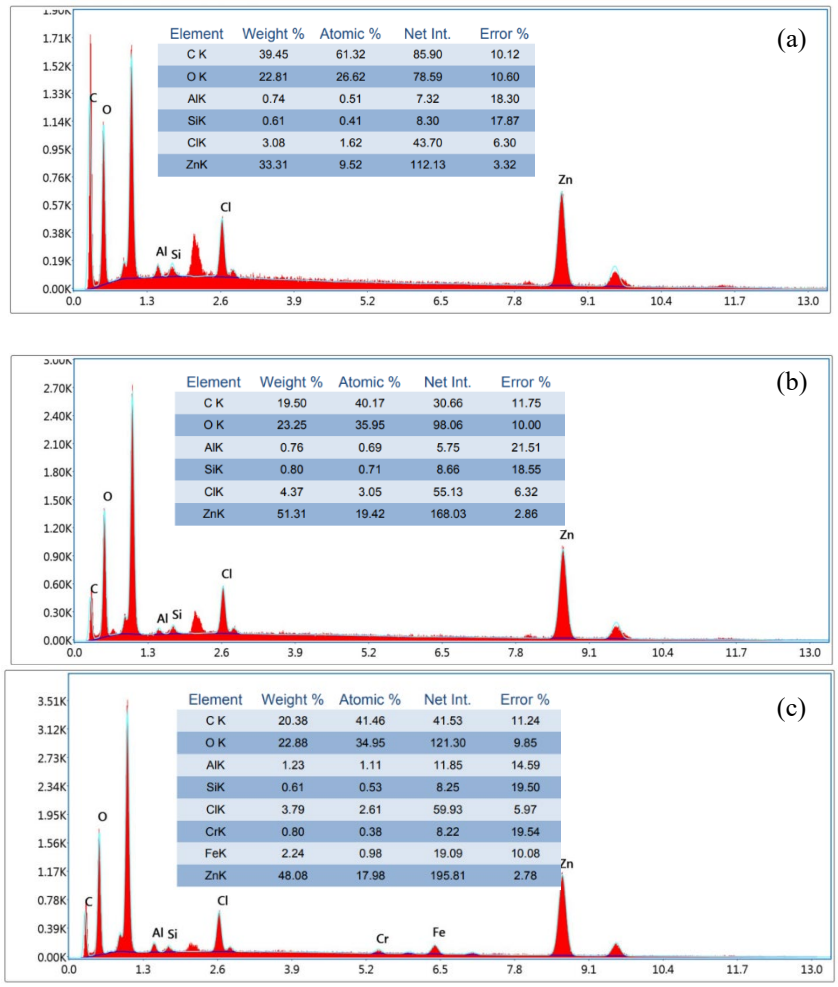

Fig. 3. SEM-EDS a) AC/ZnO 0.01 M, b) AC/ZnO 0.05 M, and c) AC/ZnO 0.1 M

In Fig. 2, there is the element Cl in a low weight percent ranging from 3-5%, indicating that Cl trapped in the carbon pores. Other elements such as Cr and Fe are among the elements found in ink or pen ink while the paper contains Si and Al. These elements have much weaker weight percent values or spectral peaks so as not to consider the presence of these elements in the activated carbon-composite examined [21]. Despite the fact that ink and other additives were eliminated from the waste paper prior to the carbonization stage, this may have happened because the ink layer's locally variable thickness is dependent on the pressure and speed used when writing or printing [21].

In each concentration of doping, it is known that AC/ZnO 0.01 M contains the largest C of 39.45%. Meanwhile, the concentrations of 0.05 M and 0.1 M have similar weight percentages of 23.25% and 22.88%. Comparably, the presence of zinc increased from 33.31% to 51.31% when the concentration of zinc acetate was raised from 0.01 M to 0.05 M. However, there was a minor drop in weight percent (48.08%) when the precursor concentration was increased by 0.1 M. If the impregnation process is carried out for two hours, with an estimated lack of maximum time given to occupy the pores of activated carbon, so that it is not perfectly impregnated, zinc loss as the precursor increases. The pH setting that is being used may also have other effects. The amount of H^+ or OH^- ions in the sol has a significant impact on the shape of metal oxide nanoparticles produced by sol-gel synthesis. During the ZnO growth process, these ions control the polymerization of metal-oxygen bonds [22].

In order to investigate the properties of AC and AC/ZnO further, XRD analysis revealed that the activated carbon obtained from waste paper was amorphous and had been effectively doped with ZnO nanoparticles. It is known that the activated carbon generated contains ZnO from the chemical activator used, namely $ZnCl_2$, based on the XRD data in Fig. 4. A reaction occurs between $ZnCl_2$ and water resulting from thermal cutting of sellulose molecules which occurs at temperatures of 240 - 400˚C. In a study conducted by Ma, et al. (2015), this reaction occurred at a temperature of 360˚C which was indicated by the appearance of the compound $Zn_2OCl_2.2H_2O$ identified by the sharp peak

of XRD at 2θ is 11.2˚ and detected ZnO peak at 2θ between 30˚ to 40˚ followed up to 59.7◦, this indicates the decomposition of $Zn_2OCl_2.2H_2O$ that can occur further when the temperature is increased to 600˚C, where the evaporation of $ZnCl_2$ occurs with the following reaction taking place on eq. (4) and (5).

$$2ZnCl_2 + 3H_2O \rightarrow Zn_2OCl_2.2H_2O + 2HCl(g) \quad (4)$$

$$Zn_2OCl_2.2H_2O \rightarrow ZnCl_2(g) + 2H_2O(g) + ZnO(s) \quad (5)$$

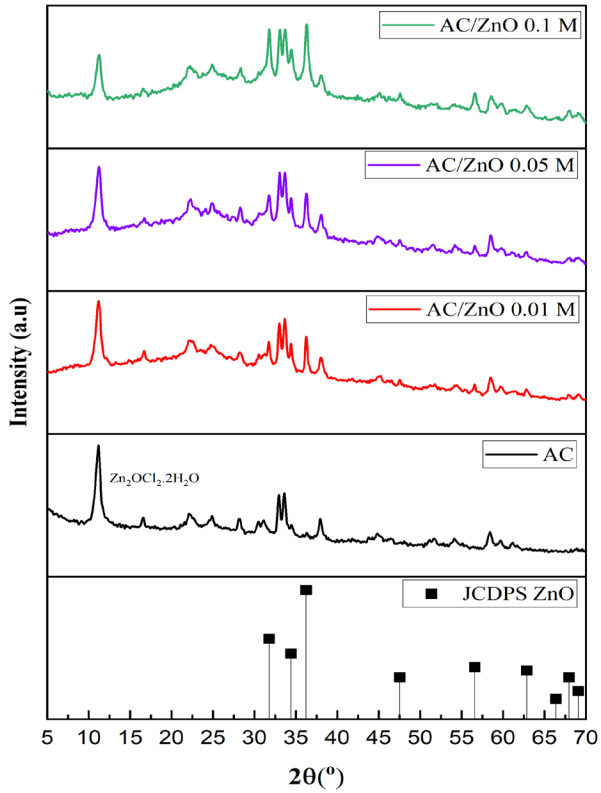

Fig. 4. Crystal phases on each variabel and JCPDS reference (036-1451)

Table 1. Calculation results ZnO crystal diameter

Name	Crystal Diameter (nm)
Activated Carbon (AC)	19.5711
AC/ZnO 0.01 M	36.8390
AC/ZnO 0.05 M	29.5939
AC/ZnO 0.1 M	27.9779

The hexagonal wurtzite (w-ZnO) shape of the ZnO particles obtained is evident from the diffraction peak data of each variable on Fig. 4, and this is the most thermodynamically stable phase of ZnO [23]. And from Table 1, it is known that activated carbon has the smallest ZnO crystal diameter compared to activated carbon doped with ZnO from zinc acetate precursor. The small crystal size results in a wide diffraction peak in this method. The width of the diffraction peak is affected by microstrain (lattice strain), which is the effect of the displacement of a unit cell around its normal position which can be caused by several things such as: (1) Non-uniform lattice distortion, which can result from nanocrystal surface tension, crystal shape morphology, and interstitial impurities. (2) Dislocations, (3) Inter-phase domain boundaries formed during the preparation of material structures that are subjected to preparation transformation disturbances [24].

The functional groups of activated carbon were studied from the results of analysis using fourier transform infrared (FTIR). The O—H stretching vibrations of carboxylic acids correspond to the broad band at about 3500 cm^{-1}. Due to the N_2 atmosphere used during the carbonization process, the peak near 1540 cm^{-1} may be related to N—H bending vibrations or C—N bending vibrations. It also corresponds to the C=C aromatic structure. The broad band at 1040 cm^{-1} in the fingerprint area represents the C—O—C stretching of cellulose and hemicellulose. The ester ether ring's C—O—C symmetry vibration is represented by the peak at 902 cm^{-1}. The broad band at 612 cm^{-1} corresponds to a C—H bend, while the peak at 707 cm^{-1} indicates C—Cl and . This suggests that the waste paper-based adsorbent's surface has a large number of functional groups.

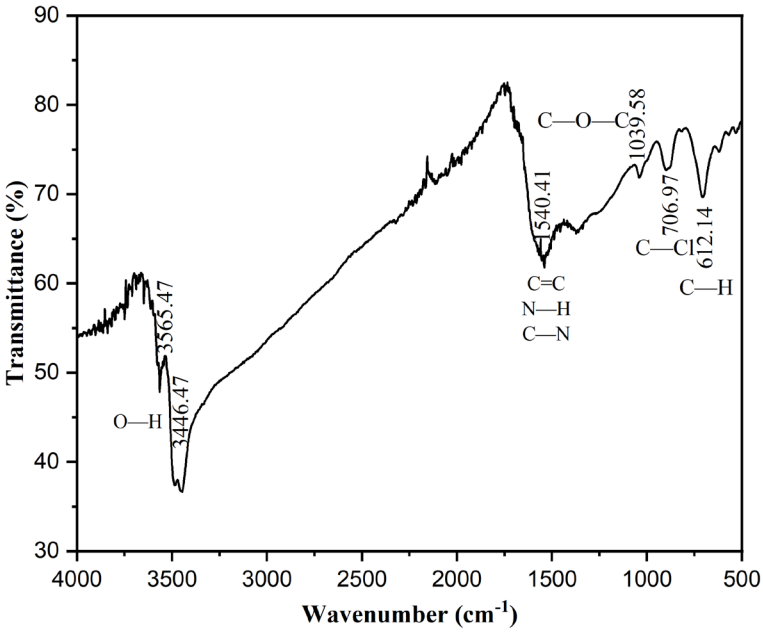

Fig. 5. FTIR of activated carbon based waste paper

Photocatalytic Activity

The synergistic effect, which combines an adsorbent and a photocatalyst, is a viable and effective method for eliminating pollutants from wastewater. When photonic energy radiation (hv) that is equal to or greater than the ZnO band gap is applied to the ZnO surface, the photocatalytic process starts [25]. Reactive species, like $OH^{\bullet}$ and $O_2^{\bullet-}$, are produced when visible or UV light interacts with catalysis. These species can then interact with organic pollutants to initiate the degradation process [26]. In our earlier study, the mechanism of photocatalytic activity was thoroughly explained [23].

One of the most effective methods is MB photodegradation since MB can also act as a photocatalyst sensitizer. Irradiation time, light intensity source, and MB concentration are factors that can affect MB photodegradation [27]. Fig. 6(c), shows that AC/ZnO 0.05 M perfectly degraded 15 mg/L (0.5 g/L) of MB at 75 min. As for the adsorption-desorption, there was a very significant increase in the degradation rate within -30 min before irradiation. This indicates that ZnO formed from the pyrolysis and doping process plays a role in the MB degradation process in the absence of light. As the irradiation time increases, the rate of degradation will also increase. As the reaction time increases, the absorption peak progressively diminishes. The dye initially shifts from dark to bright, increases progressively with longer exposure times, and eventually becomes consistent.

The photocatalytic performance of 0.05 M and 0.1 M AC/ZnO at 0.5 L/g was comparable to activated carbon. Further investigation is necessary to see the influence or differences between each particle, and the results indicate that AC/ZnO 0.05 performs better than the others, but AC catches up rather rapidly at 45 and 30 minutes with a degradation efficiency of 64.98% and 21.51%. This demonstrates that the surface area of activated carbon is greater than that of the AC/ZnO combination. Its ability to adsorb MB will be impacted when the additional concentration of zno is raised because the carbon surface's active adsorption sites would decrease [2].

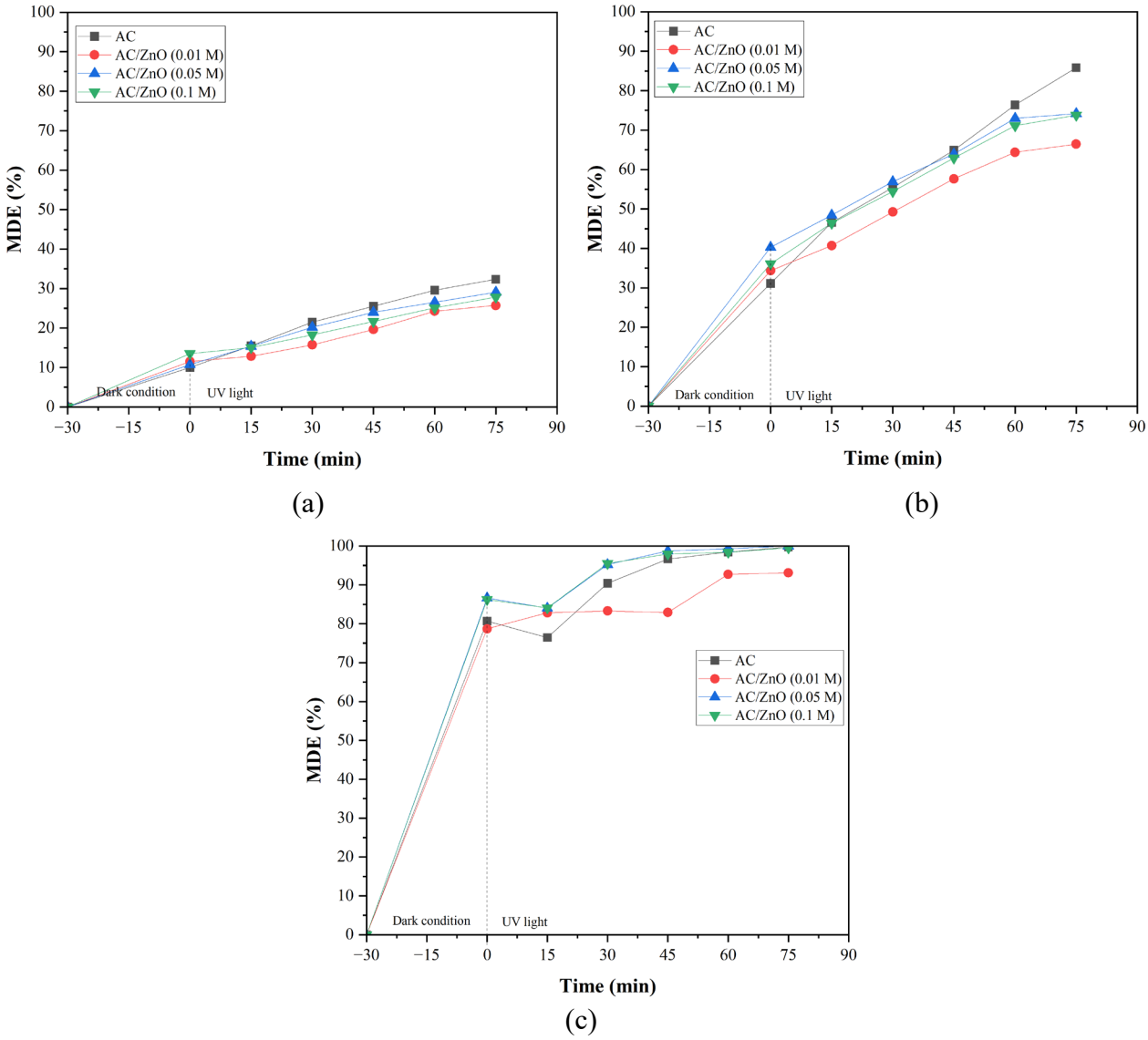

Fig. 6. AC and AC/ZnO Methylene Blue Degradation Efficiency (MDE) with varying proportions (a) 0.1 g/L, (b) 0.3 g/L, and (c) 0.5 g/L

Summary

Activated carbon was successfully made from waste paper in a single process that required an hour at a 400 °C pyrolysis temperature. ZnO at concentrations of 0.01, 0.05, and 0.1 M was synthesized from zinc acetate to conduct adsorption and photocatalytic tests. The resultant ZnO nanoparticles resembled flowers in shape. Various adsorbent loadings were used to test photocatalytic activity both with and without UV light irradiation. When methylene blue was used as a pollutant, the adsorbent-composite's photocatalytic activity led to its complete degradation by AC/ZnO 0.05 M, but for other particle mass concentration, it demonstrated how activated carbon can hinder ZnO's ability to block UV light.

Acknowledgment

With contract number 084/E5/PG.02.00.PT/2023, the writers would like to express their gratitude to DRPM Kementrian Pendidikan, Kebudayaan, Riset dan Teknologi Indonesia.

References

[1] A. Ghofur, D. A. Rachman, M. M. Lutfi, and F. Rahman, "The Influence of Leachate Water on Corrosion Rate of Mild Steel Plate," no. 7, pp. 137–143, 2021, [Online]. Available: https://doi.org/10.21776/MECHTA.2021.002.02.7%0D.

[2] G. J. F. Cruz *et al.*, "Composites of ZnO nanoparticles and biomass based activated carbon: Adsorption, photocatalytic and antibacterial capacities," *Water Sci. Technol.*, vol. 2017, no. 2, pp. 492–508, 2017, doi: 10.2166/wst.2018.176.

[3] X. Tang, G. Ran, J. Li, Z. Zhang, and C. Xiang, "Extremely efficient and rapidly adsorb methylene blue using porous adsorbent prepared from waste paper: Kinetics and equilibrium studies," *J. Hazard. Mater.*, vol. 402, no. April 2020, p. 123579, 2021, doi: 10.1016/j.jhazmat.2020.123579.

[4] J. Yu *et al.*, "Eco-friendly and facile one-step synthesis of a three dimensional net-like magnetic mesoporous carbon derived from wastepaper as a renewable adsorbent," *RSC Adv.*, vol. 9, no. 22, pp. 12419–12427, 2019, doi: 10.1039/c9ra01332f.

[5] S. N. Shintre, S. Wadhai, and P. Thakur, "Synthesis of Ag/ZnO-AC composite photocatalyst: spectroscopic investigation, parameter optimization, synergistic effect and performance enhancement for cost-effective photocatalytic degradation of phenols and dyes," *Water Sci. Technol.*, vol. 85, no. 9, pp. 2663–2681, 2022, doi: 10.2166/wst.2022.137.

[6] D. Ozdemir, "Production of activated carbon from the waste paper by chemical activation method," vol. 07, pp. 52–61, 2023, doi: 10.35860/iarej.1222591.

[7] M. Manurung, O. Ratnayani, and R. A. Prawira, "Sintesis dan Karakterisasi Arang dari Limbah Bambu," *Cakra Kim.*, vol. 7, no. 1, pp. 69–77, 2019, [Online]. Available: https://ojs.unud.ac.id/index.php/cakra/article/view/51644/30624

[8] C. Z. Zaman *et al.*, "Pyrolysis: A Sustainable Way to Generate Energy from Waste," *Pyrolysis*, pp. 3–36, 2017, doi: 10.5772/intechopen.69036.

[9] D. Zhou *et al.*, "Activated carbons prepared via reflux-microwave-assisted activation approach with high adsorption capability for methylene blue," *J. Environ. Chem. Eng.*, vol. 9, no. 1, p. 104671, 2021, doi: 10.1016/j.jece.2020.104671.

[10] W. Hu *et al.*, "Waste phenolic resin derived activated carbon by microwave-assisted KOH activation and application to dye wastewater treatment," *Green Process. Synth.*, pp. 408–415, 2019.

[11] F. Lin *et al.*, "Real-time monitoring the carbonization and activation process of activated carbon prepared from Chinese parasol via zinc chloride activation," *J. Anal. Appl. Pyrolysis*, vol. 155, no. February, p. 105089, 2021, doi: 10.1016/j.jaap.2021.105089.

[12] N. Isoda *et al.*, "Optimization of preparation conditions of activated carbon from agriculture waste utilizing factorial design," *Powder Technol.*, vol. 256, pp. 175–181, 2014, doi: 10.1016/j.powtec.2014.02.029.

[13] S. H. Abro, H. A. Moria, M. N. Alghamdi, A. Z. Al-Khazaal, and S. Saad-Ul-Haque, "Development and Characterization of Antibacterial Activated Carbon Composite of Zinc and Oxide for Water Filtration as an Industrial Application," *Pakistan J. Sci. Ind. Res. Ser. A Phys. Sci.*, vol. 63, no. 3, pp. 162–167, 2020, doi: 10.52763/pjsir.phys.sci.63.3.2020.162.167.

[14] I. Velo-Gala, J. J. López-Peñalver, M. Sánchez-Polo, and J. Rivera-Utrilla, "Activated carbon as photocatalyst of reactions in aqueous phase," *Appl. Catal. B Environ.*, vol. 142–143, pp. 694–704, 2013, doi: 10.1016/j.apcatb.2013.06.003.

[15] M. Julita, M. Shiddiq, and M. Khair, "Determination of Band Gap Energy of ZnO/Au Nanoparticles Resulting in Laser Ablation in Liquid," *Indones. J. Chem. Res.*, vol. 10, no. 2, pp. 83–87, 2022, doi: 10.30598//ijcr.2022.10-mar.

[16] K. Kusdianto, T. D. Sari, M. A. Laksono, S. Madhania, and S. Winardi, "Fabrication and application of ZnO-Ag nanocomposite materials prepared by gas-phase methods," *IOP Conf. Ser. Mater. Sci. Eng.*, vol. 1053, no. 1, p. 012023, 2021, doi: 10.1088/1757-899x/1053/1/012023.

[17] X. Zhang *et al.*, "Carbon-Doped ZnO Nanostructures: Facile Synthesis and Visible Light Photocatalytic Applications," *J. Phys. Chem. C*, vol. 119, no. 35, pp. 20544–20554, 2015, doi: 10.1021/acs.jpcc.5b07116.

[18] M. Vinayagam, S. Ramachandran, V. Ramya, and A. Sivasamy, "Photocatalytic degradation of orange G dye using ZnO/biomass activated carbon nanocomposite," *J. Environ. Chem. Eng.*, vol. 6, no. 3, pp. 3726–3734, 2018, doi: 10.1016/j.jece.2017.06.005.

[19] Rahmi and Lelifajri, "Influence of heat treatment on eggshell particles as low cost adsorbent for methylene blue removal from aqueous solution," *Rasayan J. Chem.*, vol. 10, no. 2, pp. 634–642, 2017, doi: 10.7324/RJC.2017.1021736.

[20] A. Kajbafvala, H. Ghorbani, A. Paravar, J. P. Samberg, E. Kajbafvala, and S. K. Sadrnezhaad, "Effects of morphology on photocatalytic performance of Zinc oxide nanostructures synthesized by rapid microwave irradiation methods," *Superlattices Microstruct.*, vol. 51, no. 4, pp. 512–522, 2012, doi: 10.1016/j.spmi.2012.01.015.

[21] F. Cicconi, V. Lazic, A. Palucci, A. C. A. Assis, and F. S. Romolo, "Forensic analysis of commercial inks by laser-induced breakdown spectroscopy (LIBS)," *Sensors (Switzerland)*, vol. 20, no. 13, pp. 1–20, 2020, doi: 10.3390/s20133744.

[22] S. Arya *et al.*, "Review—Influence of Processing Parameters to Control Morphology and Optical Properties of Sol-Gel Synthesized ZnO Nanoparticles," *ECS J. Solid State Sci. Technol.*, vol. 10, no. 2, p. 023002, 2021, doi: 10.1149/2162-8777/abe095.

[23] K. Kusdianto, W. Widiyastuti, M. Shimada, T. Nurtono, S. Machmudah, and S. Winardi, "Photocatalytic Activity of ZnO-Ag Nanocomposites Prepared by a One-step Process using Flame Pyrolysis," *Int. J. Technol.*, vol. 10, no. 3, pp. 571–581, May 2019, doi: https://doi.org/10.14716/ijtech.v10i3.2902.

[24] S. Speakman, "Estimating Crystallite Size Using XRD (MIT Center for Materials Science and Engineering," *Estim. Cryst. Size Using XRD (MIT Cent. Mater. Sci. Eng.*, pp. 5–15, 2008, [Online]. Available: http://prism.mit.edu/XRAY/oldsite/CrystalSize%0AAnalysis.pdf

[25] U. G. Akpan and B. H. Hameed, "Parameters affecting the photocatalytic degradation of dyes using TiO2-based photocatalysts: A review," *J. Hazard. Mater.*, vol. 170, no. 2–3, pp. 520–529, 2009, doi: 10.1016/j.jhazmat.2009.05.039.

[26] M. A. Fagier, "Plant-Mediated Biosynthesis and Photocatalysis Activities of Zinc Oxide Nanoparticles: A Prospect towards Dyes Mineralization," *J. Nanotechnol.*, vol. 2021, 2021, doi: 10.1155/2021/6629180.

[27] I. Khan *et al.*, "Review on Methylene Blue: Its Properties, Uses, Toxicity and Photodegradation," *Water (Switzerland)*, vol. 14, no. 2, 2022, doi: 10.3390/w14020242.